Particles with an Undulated Contact Line at a Fluid Interface: Interaction between Capillary Quadrupoles and Rheology of Particulate Monolayers

Peter A. Kralchevsky,* Nikolai D. Denkov, and Krassimir D. Danov

Laboratory of Chemical Physics and Engineering, Faculty of Chemistry, University of Sofia, 1, J. Bourchier Avenue, Sofia 1164, Bulgaria

Received June 20, 2001. In Final Form: August 28, 2001

We consider solid particles attached to a liquid−fluid interface. If the solid−liquid−fluid contact line (at the particle surface) is undulated, the convex and concave local deviations of the meniscus shape from planarity can be treated as positive and negative capillary charges, which form capillary multipoles. Correspondingly, the meniscus shape can be expressed as a multipole expansion. The leading terms of the capillary multipole expansion turn out to be the charges and quadrupoles. In the present article, we derive theoretical expressions, which enable one to calculate the energy and force of interaction between two capillary quadrupoles for arbitrary interparticle distance. Depending on the amplitudes of the contact-line undulations, and on the particle mutual orientations, the interaction is either monotonic attraction or attraction at long distances but repulsion at short distances. As a rule, the interaction energy is much larger than the thermal energy kT, even for undulations of nanometer amplitudes. This implies the existence of a specific rheological behavior of adsorption monolayers made of such particles. For example, an equilibrium monolayer of identical particles exhibits a plastic behavior upon dilatation; an expression for the respective yield stress is derived. In addition, expressions for the contributions of the capillary interactions to the surface dilatational and shear modules of elasticity are derived. The results of this paper could be helpful for the understanding of some phenomena related to the aggregation and the ordering of particles adsorbed at a fluid interface and for the interpretation of the rheological behavior of monolayers from such particles.

1. Introduction

1.1. Capillary Charges. Many processes and phenomena (such as the known capillary rise) are caused by the action of capillary forces, which are related to the interfacial tension of fluid phase boundaries. Here we use the term "capillary forces" in a narrower sense, viz. as interactions between particles mediated by fluid interfaces. The origin of the lateral capillary forces is the overlap of perturbations in the shape of a liquid surface which is caused by the presence of attached particles. The larger the interfacial deformation created by the particles is, the stronger the capillary interaction is between them.[1−8] It is known that two similar particles floating on a liquid interface attract each other (Figure 1a). The attraction appears because the gravitational potential energy of the two particles decreases when they approach each other. Hence, the origin of this flotation capillary force is the particle weight (including the buoyancy force).[1−5] Capillary interaction appears also when the particles (instead of being freely floating) are partially immersed (confined) in a liquid layer; this is the immersion capillary force (Figure 1c).[5,6] The deformation of the liquid surface in this case is related to the wetting properties of the particle surface, that is, to the position of the contact line and the magnitude of the contact angle, rather than to gravity. The flotation and immersion forces can be attractive or repulsive (for detailed reviews see refs 7 and 8).

For the systems depicted in Figure 1a and c, by solving the Laplace equation of capillarity for a small meniscus slope, $\nabla^2\zeta = q^2\zeta$, in cylindrical coordinates (r,φ), one can determine the interfacial shape around a single particle with a circular contact line of radius r_1:

$$\zeta(r) = Q_1 K_0(qr) \tag{1.1}$$

ζ is the deviation of the fluid interface from planarity (Figure 1a); K_0 is the modified Bessel function of the second kind and zeroth order; $Q_1 = r_1 \sin(\psi_1)$, where ψ_1 is the meniscus slope angle at the contact line; $q^2 = \Delta\rho g/\sigma$, where $\Delta\rho$ is the difference between the mass densities of the lower and upper fluids, σ is the interfacial tension of the boundary between them, g is the acceleration due to gravity, and, in thin liquid films, q is related to the disjoining pressure rather than to gravity.[5−8] The presumption for small slope, used to linearize the Laplace equation, means that $|\nabla\zeta|^2 \ll 1$. In the case of the floating particle of radius R_1, the fulfillment of the latter presumption can be verified with the help of the following relationship:

$$|\nabla\zeta| \leq \frac{q^2 {R_1}^3}{6r_1}|2 - 4D_1 + 3\cos(\alpha_1) - \cos^3(\alpha_1)| \tag{1.2}$$

which stems from eqs 8.5 and 8.16 in ref 8. Here α_1 is the three-phase contact angle measured across the lower fluid; $D_1 = (\rho_1 - \rho_{up})/\Delta\rho$, where ρ_1 and ρ_{up} are the mass densities of the floating particle and the upper fluid.

* To whom correspondence should be addressed. E-mail: pk@ltph.bol.bg.

(1) Nicolson, M. M. *Proc. Cambridge Philos. Soc.* **1949**, *45*, 288.
(2) Chan, D. Y. C.; Henry, J. D.; White, L. R. *J. Colloid Interface Sci.* **1981**, *79*, 410.
(3) Paunov, V. N.; Kralchevsky, P. A.; Denkov, N. D.; Nagayama, K. *J. Colloid Interface Sci.* **1993**, *157*, 100.
(4) Allain, C.; Cloitre, M. *J. Colloid Interface Sci.* **1993**, *157*, 261; 269.
(5) Kralchevsky, P. A.; Nagayama, K. *Langmuir* **1994**, *10*, 23.
(6) Kralchevsky, P. A.; Paunov, V. N.; Ivanov, I. B.; Nagayama, K. *J. Colloid Interface Sci.* **1992**, *151*, 79.
(7) Kralchevsky, P. A.; Nagayama, K. *Adv. Colloid Interface Sci.* **2000**, *85*, 145.
(8) Kralchevsky, P. A.; Nagayama, K. *Particles at Fluid Interfaces and Membranes*; Elsevier: Amsterdam, 2001.

10.1021/la0109359 CCC: $20.00
Published on Web 11/03/2001

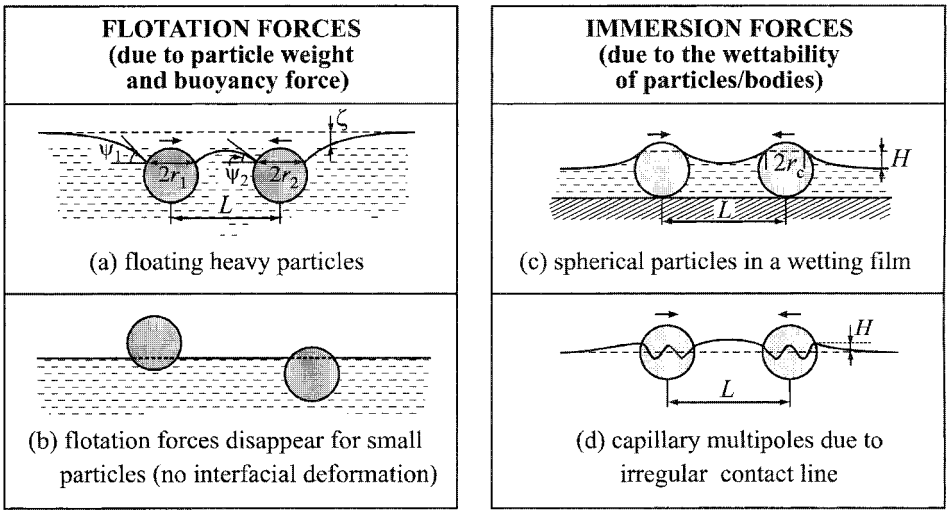

Figure 1. Types of capillary forces between particles captive at an interface. **(a)** Flotation force: the deformations are caused by the particle weight and buoyancy; (b) this force disappears if the particle weight is insufficient to deform the fluid interface. (c,d) Immersion force: the deformations stem from the position and shape of the contact line and magnitude of the contact angle. (c) If the deformation around an isolated particle is axisymmetric, we deal with capillary charges. (d) The forces between particles of an undulated or irregular contact line can be described as interactions between capillary multipoles, in analogy with electrostatics.

Further, one can apply Nicolson's[1] superposition approximation, that is, assume that the interfacial deformation caused by two particles (Figure 1a,c) is equal to the sum of the axisymmetric deformations caused by the separate particles in isolation. In view of eq 1.1, the energy of lateral capillary interaction between the two particles can then be obtained in the form[2,3,5,7,8]

$$\Delta W \approx -2\pi\sigma Q_1 Q_2 K_0(qL) \qquad (1.3)$$

where L denotes the distance between the centers of the two particles, and $Q_i \equiv r_i \sin(\psi_i)$ $(i = 1,2)$ are the so-called "capillary charges",[3,5] where r_i and ψ_i are the radius of the contact line and the slope angle at the contact line of the respective particle (see Figure 1a for the notation). (The use of superposition approximation can be avoided by employing bipolar coordinates; see section 3.1.) The lateral capillary force is given by the derivative $F = -\mathrm{d}\Delta W/\mathrm{d}L$, which yields[2,3,5,7,8]

$$F \approx -2\pi\sigma Q_1 Q_2 q K_1(qL), \quad (r_k \ll L) \qquad (1.4)$$

(K_1: modified Bessel function). The asymptotic form of eq 1.4 for $qL \ll 1$ ($q^{-1} = 2.7$ mm for water),

$$F = -2\pi\sigma Q_1 Q_2/L, \quad (r_k \ll L \ll q^{-1}) \qquad (1.5)$$

looks like a two-dimensional analogue of Coulomb's law for the electrostatic force would; this is the reason to call Q_1 and Q_2 capillary charges. Generally speaking, the capillary charge characterizes the local deviation of the meniscus shape from planarity at the three-phase contact line. The flotation and immersion capillary forces exhibit similar dependence on the interparticle separation, L, but very different dependencies on the particle radius and the surface tension of the liquid. For example, in the case of two identical spherical particles of radius R, one has $F_{\mathrm{immersion}} \propto R^2\sigma$, whereas $F_{\mathrm{flotation}} \propto R^6/\sigma$ (see refs 5, 7, and 8 for details).

1.2. Capillary Multipoles. The analogy between the capillary and electrostatic interactions can be extended further; in addition to the immersion force between capillary charges (monopoles), one can also introduce immersion forces between "capillary multipoles". Indeed, the weight of a floating micrometer-sized (or submicrometer) particle is too small to create any surface deformation (Figure 1b). This is related to the fact that $F_{\mathrm{flotation}} \propto R^6$, and consequently, the flotation force strongly decreases and vanishes with diminishing particle size. However, surface deformations could appear even with such small particles if the contact line on the particle surface is irregular (say, undulated as in Figure 1d), rather than a circular three-phase line of contact. For example, this may happen in the cases of angular or irregular particle shape, presence of surface roughness, chemical inhomogeneity, etc. In such cases, instead of eq 1.1, the meniscus shape around a single particle is described by the expression

$$\zeta(r,\varphi) = \sum_{m=1}^{\infty} K_m(qr)(A_m \cos(m\varphi) + B_m \sin(m\varphi)) \qquad (1.6)$$

which is the respective solution of the linearized Laplace equation of capillarity for a small meniscus slope, $\nabla^2\zeta = q^2\zeta$, in cylindrical coordinates (r,φ). Here A_m and B_m are constants of integration. For $qr \ll 1$, one has $K_m(qr) \propto (qr)^{-m}$, and then eq 1.6 reduces to a multipole expansion (a two-dimensional analogue of that in electrostatics). The terms with $m = 1, 2, 3,...$ correspond to dipole, quadrupole, hexapole, etc. Such multipoles have been observed in experiments by Bowden et al.[9,10] who used appropriate hydrophobization or hydrophilization of the sides of floating hexagonal plates (see also ref 11).

From a theoretical viewpoint, the capillary force between particles of an irregular or undulated contact line could be considered as a kind of immersion force insofar as it is related to the particle wettability, rather than to the particle weight. Equation 1.1 is the zeroth-order term of the expansion in eq 1.6. For $m \geq 1$, the capillary force can cause not only translation, but also rotation of the particles.

Lucassen[12] was the first to develop a quantitative theory of the capillary forces between particles with an undulated

(9) Bowden, N.; Terfort, A.; Carbeck, J.; Whitesides, G. M. *Science* **1997**, *276*, 233.
(10) Bowden, N.; Choi, I. S.; Grzybowski, B. A.; Whitesides, G. M. *J. Am. Chem. Soc.* **1999**, *121*, 5373.
(11) Kralchevsky, P. A.; Denkov, N. D. *Curr. Opin. Colloid Interface Sci.* **2001**, *6*, 383.
(12) Lucassen, J. *Colloids Surf.* **1992**, *65*, 131.

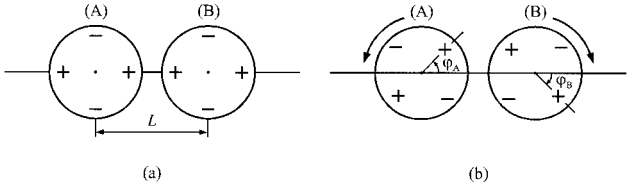

Figure 2. Sketch of two particles, capillary quadrupoles, A and B, separated at a distance L. The signs "+" and "−" symbolize convex and concave local deviations of the contact line from planarity. (a) Initial state. (b) After rotation of the respective particles at angles φ_A and $\varphi_B = -\varphi_A$.

contact line. He considered "rough-edged" cubic particles with a sinusoidal contact line. The calculated capillary force exhibits a minimum; it is attractive at long distances and repulsive at short separations. Any interfacial deformation, either by dilatation or by shear, takes the particles out of their equilibrium positions (at the minimum) and is, therefore, resisted. As a consequence, the particulate monolayer exhibits elastic properties.[12] Expressions for the surface dilatational and shear elastic moduli have been derived in refs 8 and 12.

A theoretical description of the lateral capillary force between colloidal spheres of an undulated contact line was recently given by Stamou et al.[13] These authors note that if the particles are freely floating, then the capillary force will spontaneously rotate each particle around a horizontal axis to annihilate the capillary dipole moment (unless the particle rotation is hindered, e.g., by a solid substrate). Therefore, the term with $m = 1$ in eq 1.6 has to be skipped, and the leading multipole order in the capillary force between two such particles is the quadrupole−quadrupole interaction ($m = 2$); the respective interaction energy is[13]

$$\Delta W(L) = -12\pi\sigma H^2 \cos(2\varphi_A + 2\varphi_B)\frac{r_c^4}{L^4} \quad (m = 2;\ L \gg 2r_c) \quad (1.7)$$

where H is the amplitude of the undulation of the contact line, whose average radius is r_c; the angles φ_A and φ_B are subtended between the diagonals of the respective quadrupoles and the line connecting the centers of the two particles. For two particles in contact ($L/r_c = 2$) and optimal orientation, $\cos(2\varphi_A + 2\varphi_B) = 1$, one obtains $\Delta W = -(3/4)\pi\sigma H^2$. Thus, for interfacial tension $\sigma = 35$ mN/m, the interaction energy ΔW becomes greater than the thermal energy kT for an undulation amplitude $H > 2.2$ Å. This result is really astonishing; even a minimal roughness of the contact line could be sufficient to give rise to a significant capillary attraction, which may produce 2-D aggregation of colloidal particles attached to a fluid interface[13] (see also refs 11, 12, and Chapter 12 in ref 8).

Figure 2 shows a top view of two particles−quadrupoles, denoted A and B; the shape of their contact lines is determined by the expression

$$\zeta_Y(\varphi) = H_Y \cos(2\varphi - 2\varphi_Y), \quad Y = \text{A, B} \qquad (1.8)$$

where H_A and H_B are the amplitudes of the contact line undulations. Since similar (opposite) capillary charges attract (repel) each other, the configuration depicted in Figure 2a corresponds to an equilibrium mutual angular orientation (L is fixed). If the particles are rotated at equal angles in the opposite directions (Figure 2b), that is, $\varphi_A = -\varphi_B$, then $\cos(2\varphi_A + 2\varphi_B) = 1$, and eq 1.7 predicts that the interaction energy $\Delta W(L)$ remains constant during such a rotation.

Note that in eq 1.8 (and hereafter in this paper), it is assumed that the three-phase contact line is fixed to an edge on the particle surface, which is undulated because of surface roughness or inhomogeneity. In such a case, the contact angle exhibits a large hysteresis and does not take a fixed value.[8] The physical parameter, which enters the boundary condition at the contact line, and therefrom is the theoretical expression for ΔW, is the amplitude of undulation, H_Y, rather than the contact angle.

For multipoles, the sign and magnitude of the capillary force depend on the particle mutual orientation. For that reason, particles−quadrupoles ($m = 2$) will tend to assemble in a square lattice, whereas particles−hexapoles ($m = 3$) will preferably form a hexagonal lattice, with or without voids.[11] Such lattices (hexagonal with voids and square) have been observed experimentally.[9,10]

1.3. Aim and Structure of the Paper. In this article, we address the problem of the interactions between capillary quadrupoles because of the following several reasons: (i) As mentioned above, for micrometer- and submicrometer-sized particles, the flotation force (equivalent to interaction between capillary charges) disappears (Figure 1b). Moreover, the capillary dipoles are spontaneously annihilated. Then the quadrupole becomes the leading term in the capillary multipole expansion. (ii) As discussed after eq 1.7, the quadrupole−quadrupole interaction is considerable and deserves special attention. Such an interaction has been observed in the experiments by Bowden et al.[9,10] (iii) Equation 1.7 is an asymptotic expression for $\Delta W(L)$, which is correct only for large distances between two capillary quadrupoles, $L \gg 2r_c$. Our purpose here is to calculate $\Delta W(L)$ for the arbitrary interparticle distance $L \in [2r_c, \infty)$ in the general case of different undulation amplitudes, that is for $H_A \neq H_B$. (iv) Our aim is also to determine theoretically the rheological response of an equilibrium monolayer of particles−quadrupoles subjected to dilatational and shear surface deformations. The detection of surface shear and/or dilatational elasticity with particulate adsorption monolayers can indicate the presence of interactions between capillary quadrupoles.

With regard to the higher-order terms in multipole expansion 1.6, such as hexapoles, etc., their interactions might be considerable at smaller L or when there is no quadrupole moment, as in some model experiments.[9,10] The hexapole−hexapole interaction could be a subject of a subsequent study.

The paper is organized as follows. In section 2, we introduce the basic equations. In section 3, we derive an explicit expression for the calculation of $\Delta W(L)$ by solving the respective boundary problem using bipolar coordinates. Next, we present and discuss the numerical results for the interaction energy and force. Finally, we derive expressions for some rheological properties of an adsorption monolayer formed by particles−quadrupoles: yield stress and surface shear elasticity.

The theoretical approach developed in this article can be further extended to describe the interactions between capillary multipoles of other orders and to predict the rheological behavior of monolayers formed by such particles.

2. Basic Equations

We consider two solid particles, A and B, which are attached to a planar fluid−liquid interface. The contact

(13) Stamou, D.; Duschl, C.; Johannsmann, D. *Phys. Rev. E: Stat. Phys., Plasmas, Fluids, Relat. Interdiscip. Top.* **2000**, *62*, 5263.

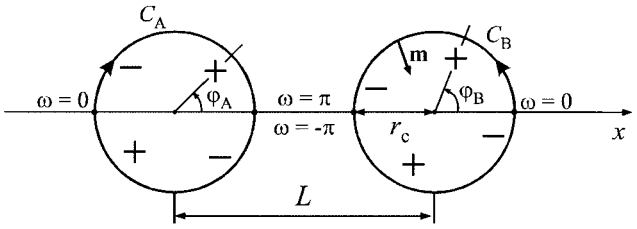

Figure 3. Sketch of two capillary quadrupoles, A and B, separated at a distance L for an arbitrary mutual orientation characterized by the angles φ_A and φ_B; C_A and C_B denote the projections of the respective contact lines on the xy plane. The angle ω of the bipolar coordinates varies in opposite directions along C_A and C_B.

lines are assumed to have a quadrupolar undulation (see eq 1.8); the projections of the contact lines in the plane of the fluid interface, C_A and C_B in Figure 3, are circumferences of radius r_c. Moreover, the weight of the particles is presumably sufficiently small so as not to produce any significant interfacial deformation. Hence, only the undulation of the contact lines is a source of interfacial deformations, which decay with the increase of the distance from the particle. The shape $z = \zeta_Y(r,\varphi)$ of the meniscus around an isolated capillary quadrupole is[13]

$$\zeta_Y = H_Y \cos[2(\varphi - \varphi_Y)]\frac{r_c^2}{r^2}, \quad Y = \text{A, B} \tag{2.1}$$

In general, the meniscus shape satisfies the Laplace equation of capillarity,

$$\nabla^2\zeta = 0 \tag{2.2}$$

which is linearized for a small meniscus slope:

$$|\nabla\zeta|^2 \ll 1, \quad \nabla \equiv \mathbf{e}_x\frac{\partial}{\partial x} + \mathbf{e}_y\frac{\partial}{\partial y} \tag{2.3}$$

where ∇ is the two-dimensional gradient operator, and $\mathbf{e}_x$ and $\mathbf{e}_y$ are the unit vectors of the Cartesian coordinate system in the plane xy, which coincides with the nondisturbed fluid interface. The meniscus excess surface energy, due to the deformation, is[6,13]

$$W(L) = \sigma\int_{S_m} \mathrm{d}s[(1 + |\nabla\zeta|^2)^{1/2} - 1] \approx \frac{\sigma}{2}\int_{S_m} \mathrm{d}s|\nabla\zeta|^2 \tag{2.4}$$

where σ is the interfacial tension, S_m is the orthogonal projection of the meniscus on the plane xy, and ds is the surface element. Next, we make the following transformation:

$$\nabla\cdot(\zeta\nabla\zeta) = (\nabla\zeta)\cdot\nabla\zeta + \zeta\nabla^2\zeta = |\nabla\zeta|^2 \tag{2.5}$$

where at the last step we have used eq 2.2. Further, we combine eqs 2.4 and 2.5 and apply the Green theorem[14]

$$W(L) = \frac{\sigma}{2}\int_{S_m} \mathrm{d}s\nabla\cdot(\zeta\nabla\zeta) = \frac{\sigma}{2}\sum_{Y=\text{A,B}}\oint_{C_Y} \mathrm{d}l\ \mathbf{m}\cdot(\zeta\nabla\zeta) \tag{2.6}$$

where dl is the linear element along the contours C_A and C_B (Figure 3), and $\mathbf{m}$ is an inner unit normal to the respective contour.

(14) McConnell, A. J. *Application of Tensor Analysis*; Dover: New York, 1957.

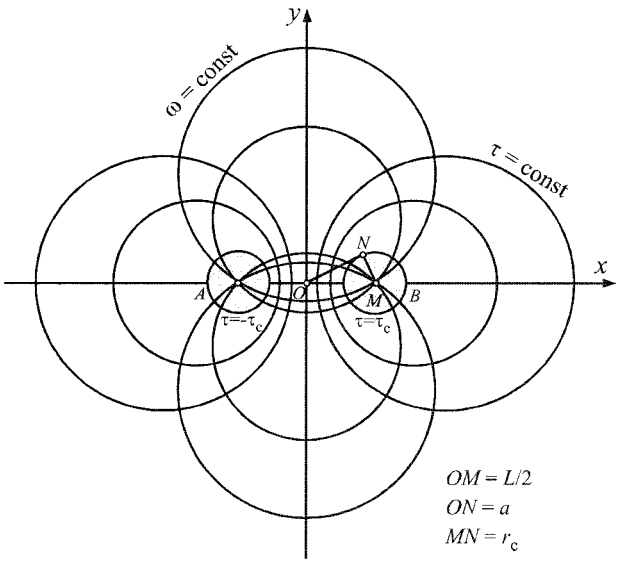

Figure 4. Bipolar coordinates (τ,ω) in the xy plane. The τ = const and ω = const coordinate lines represent two families of mutually orthogonal circumferences. The contact line projections, C_A and C_B, correspond to $\tau = \pm\tau_c$.

In the limiting case of large interparticle separation, $L \to \infty$, one can calculate the meniscus surface energy by substituting eq 2.1 into eq 2.6 (see ref 13):

$$W(\infty) = \pi\sigma(H_A^2 + H_B^2) \tag{2.7}$$

3. Meniscus Shape and Interaction Energy

3.1. Bipolar Coordinates. To obtain an explicit expression for $W(L)$, we use bipolar coordinates in the plane xy (see, e.g., ref 15), which correspond to the geometry of the system. These coordinates, denoted τ and ω, are defined through the following set of equations:

$$x = \chi\sinh(\tau), \quad y = \chi\sin(\omega), \quad \chi = a/(\cosh(\tau) - \cos(\omega)) \tag{3.1}$$

The lines τ = const and ω = const are two families of mutually orthogonal circumferences (Figure 4). In eq 3.1, a is a parameter related to the radius of the contact line and to the distance between the two particles, L (see the triangle OMN in Figure 4):

$$(L/2)^2 - a^2 = r_c^2 \tag{3.2}$$

In bipolar coordinates, eq 2.2 acquires the form

$$\frac{\partial^2\zeta}{\partial\tau^2} + \frac{\partial^2\zeta}{\partial\omega^2} = 0 \tag{3.3}$$

The use of bipolar coordinates makes the solution of the boundary problem easier because the contours C_A and C_B are simply represented by $\tau = \pm\tau_c$, with

$$\tau_c = \operatorname{arccosh}[L/(2r_c)], \quad \operatorname{arccosh}(x) = \ln[x + (x^2 - 1)^{1/2}] \tag{3.4}$$

Note also that

$$L/(2r_c) = \cosh(\tau_c), \quad a/r_c = \sinh(\tau_c) \tag{3.5}$$

(15) Korn, G. A.; Korn, T. M. *Mathematical Handbook*; McGraw-Hill: New York, 1968.

(Substitution of eq 3.5 into eq 3.2 yields the known identity $\cosh^2(\tau_c) - \sinh^2(\tau_c) = 1$.) Introducing the bipolar coordinates in eq 2.6 results in

$$W(L) = \frac{\sigma}{2}\int_{-\pi}^{\pi} d\omega\ \zeta(\omega,\tau_c)\left.\frac{\partial\zeta}{\partial\tau}\right|_{\tau=\tau_c} - \frac{\sigma}{2}\int_{-\pi}^{\pi} d\omega\ \zeta(\omega,-\tau_c)\left.\frac{\partial\zeta}{\partial\tau}\right|_{\tau=-\tau_c} \quad (3.6)$$

We seek the solution of eq 3.3 in the form of a Fourier expansion:

$$\zeta(\tau,\omega) = \sum_{n=1}^{\infty}(C_n\cos(n\omega) + D_n\sin(n\omega))\sinh[n(\tau+\tau_c)] + \sum_{n=1}^{\infty}(E_n\cos(n\omega) + F_n\sin(n\omega))\sinh[n(\tau-\tau_c)] \quad (3.7)$$

where C_n, D_n, E_n, and F_n are coefficients to be determined from the boundary conditions. By substituting eq 3.7 into eq 3.6, after some mathematical transformations, one obtains

$$W = (1/2)\pi\sigma\sum_{n=1}^{\infty} n[(C_n^2 + D_n^2 + E_n^2 + F_n^2)\cosh(2n\tau_c) + 2(C_nE_n + D_nF_n)]\sinh(2n\tau_c) \quad (3.8)$$

3.2. Determination of Unknown Coefficients. The boundary condition 1.8 yields

$$\zeta|_{\tau=-\tau_c} = H_A(\cos(2\varphi_A)\cos(2\varphi) + \sin(2\varphi_A)\sin(2\varphi)) \quad (3.9)$$

$$\zeta|_{\tau=+\tau_c} = H_B(\cos(2\varphi_B)\cos(2\varphi) + \sin(2\varphi_B)\sin(2\varphi)) \quad (3.10)$$

Next, we represent $\cos(2\varphi)$ and $\sin(2\varphi)$ as Fourier expansions with respect to ω:

$$\cos(2\varphi) = \frac{1}{\pi}\sum_{n=1}^{\infty}A_n\cos(n\omega), \quad \sin(2\varphi) = \frac{1}{\pi}\sum_{n=1}^{\infty}B_n\sin(n\omega) \quad (3.11)$$

where

$$A_n = \int_{-\pi}^{\pi}\cos(2\varphi)\cos(n\omega)\,d\omega \qquad B_n = \int_{-\pi}^{\pi}\sin(2\varphi)\sin(n\omega)\,d\omega \quad (3.12)$$

The relationship between the angles φ and ω is

$$\sin(\varphi) = \frac{\sinh(\tau_c)\sin(\omega)}{\cosh(\tau_c) - \cos(\omega)} \quad (3.13)$$

The latter equation follows from the expression $y = r_c\sin(\varphi)$, where y is substituted from eq 3.1, along with eq 3.5 for a/r_c. With the help of eqs 3.12 and 3.13, one obtains (see Appendix A)

$$A_n = \pm B_n = 4\pi\sinh(\tau_c)(n\sinh(\tau_c) - \cosh(\tau_c))\exp(-n\tau_c) \quad (3.14)$$

where the sign before B_n is "+" for the right-hand-side particle and "−" for the left-hand-side particle. Next, we set $\tau = \pm\tau_c$ in eq 3.7 and compare the result with eqs 3.9 and 3.10. Thus, in view of eqs 3.11 and 3.14, one obtains

$$C_n = H_B\frac{A_n\cos(2\varphi_B)}{\pi\sinh(2n\tau_c)}, \quad D_n = H_B\frac{A_n\sin(2\varphi_B)}{\pi\sinh(2n\tau_c)} \quad (3.15)$$

$$E_n = -H_A\frac{A_n\cos(2\varphi_A)}{\pi\sinh(2n\tau_c)}, \quad F_n = H_A\frac{A_n\sin(2\varphi_A)}{\pi\sinh(2n\tau_c)} \quad (3.16)$$

At last, the substitution of eqs 3.15 and 3.16 into eq 3.8 yields the sought-for expression for the surface excess energy $W(L)$:

$$\frac{W(L)}{\pi\sigma} = (H_A^2 + H_B^2)S(\tau_c) - H_AH_BG(\tau_c)\cos(2\varphi_A + 2\varphi_B) \quad (3.17)$$

where

$$S(\tau_c) = \sum_{n=1}^{\infty}\frac{nA_n^2}{2\pi^2}\coth(2n\tau_c) \quad (3.18)$$

$$G(\tau_c) = \sum_{n=1}^{\infty}\frac{nA_n^2}{\pi^2\sinh(2n\tau_c)} \quad (3.19)$$

τ_c is related to L by eq 3.4, and A_n is given by eq 3.14. The energy of lateral capillary interaction is

$$\Delta W(L) = W(L) - W(\infty) \quad (3.20)$$

where $W(\infty)$ is given by eq 2.7. Equations 3.17−3.20 determine the capillary interaction energy $\Delta W(L)$ for the arbitrary interparticle distance, $2r_c \le L < \infty$.

4. Numerical Results and Discussion

4.1. Functions $S(\tau_c)$ and $G(\tau_c)$. Below we investigate the series 3.18 and 3.19 to obtain the most convenient way for their summation. It will be shown that, in fact, they represent the multipole expansion for the capillary interaction between the particles depicted in Figure 3. With this end in view, let us introduce the notation

$$\epsilon \equiv \exp(-2\tau_c) \quad (4.1)$$

With the help of eq 3.4, ϵ can be expressed in the form

$$\epsilon = \frac{1}{[x + (x^2-1)^{1/2}]^2}, \quad x = \frac{L}{2r_c} \quad (4.2)$$

For long interparticle distances, eq 4.2 yields

$$\epsilon = \left(\frac{r_c}{L}\right)^2 + O(x^{-4}) \qquad (L \gg r_c) \quad (4.3)$$

The latter equation shows that the series expansion for $\epsilon \ll 1$ corresponds to a multipole expansion for large interparticle distances.

By using eqs 3.14, 3.18, 3.19, and 4.1, one can express the functions $S(\tau_c)$ and $G(\tau_c)$ in terms of ϵ:

$$S(\tau_c) = (1/2)(1-\epsilon)^2\sum_{n=1}^{\infty}n[n-1-(n+1)\epsilon]^2\epsilon^{n-2}\left(1 + \frac{2\epsilon^{2n}}{1-\epsilon^{2n}}\right) \quad (4.4)$$

Table 1. Series Expansions of $S(\tau_c)$ and $G(\tau_c)$ in Terms of the Powers of ϵ

$$S(\tau_c) = 1 + 4\epsilon^3 - 6\epsilon^4 - 8\epsilon^5 + 36\epsilon^6 - 28\epsilon^7 - 60\epsilon^8 + 148\epsilon^9 - 72\epsilon^{10} - 184\epsilon^{11} + O(\epsilon^{12})$$
$$G(\tau_c) = 12\epsilon^2 - 48\epsilon^3 + 128\epsilon^4 - 256\epsilon^5 + 440\epsilon^6 - 720\epsilon^7 + 1112\epsilon^8 - 1552\epsilon^9 + 2060\epsilon^{10} - 2832\epsilon^{11} + O(\epsilon^{12})$$

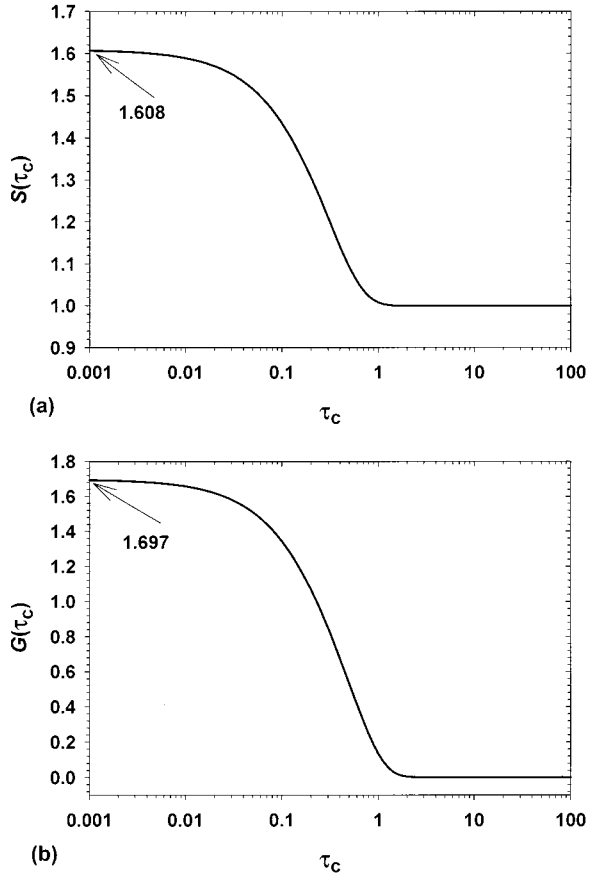

Figure 5. Computed graphs of the functions (a) $S(\tau_c)$ and (b) $G(\tau_c)$, defined by eqs 4.4 and 4.5, along with eq 4.1.

$$G(\tau_c) = (1-\epsilon)^2 \sum_{n=1}^{\infty} n[n-1-(n+1)\epsilon]^2 \frac{2\epsilon^{2n-2}}{1-\epsilon^{2n}} \quad (4.5)$$

Equations 4.4 and 4.5 are convenient for numerical computation of the functions $S(\tau_c)$ and $G(\tau_c)$. Calculated curves are shown in Figure 5. The computation becomes time-consuming for $\tau_c \to 0$, that is for $\epsilon \to 1$ (close approach of the two particles). In this limit, one can set $\epsilon = 1 - \delta$ and substitute $u = n\delta$. Then the transition $\delta \to 0$ transforms the sums in eqs 4.4 and 4.5 into integrals:

$$S(0) = (1/2)\int_0^\infty (u-2)^2 \, e^{-u} \coth(u) u \, du = 1.608\,4724... \quad (4.6)$$

$$G(0) = \int_0^\infty (u-2)^2 \frac{e^{-u}}{\sinh(u)} u \, du = 1.697\,4968... \quad (4.7)$$

As seen in Figure 5, in the opposite limit, $\tau_c \to \infty$ (long interparticle distances), $S(\tau_c) \to 1$ and $G(\tau_c) \to 0$. The asymptotic behavior in this limit can be obtained by expanding in eqs 4.4 and 4.5 for small ϵ:

$$S(\tau_c) = 1 + 4\epsilon^3 + O(\epsilon^4) \quad (4.8)$$

$$G(\tau_c) = 12\epsilon^2 - 48\epsilon^3 + O(\epsilon^4) \quad (4.9)$$

The 10-term expansions of $S(\tau_c)$ and $G(\tau_c)$, which are related to the multipole expansion for the particles in Figure 3, are given in Table 1. By substituting eqs 4.8 and 4.9 into eq 3.17, and by using eqs 2.7, 3.20, and 4.3, one obtains the asymptotic equation

$$\Delta W(L) = -12\pi\sigma H_A H_B \cos(2\varphi_A + 2\varphi_B)\frac{r_c^4}{L^4} + O(\epsilon^3) \quad (L \gg 2r_c) \quad (4.10)$$

For $H_A = H_B = H$, eq 4.10 coincides with the asymptotic eq 1.7 derived by Stamou et al.[13] As expected, the leading term in the multipole expansion of ΔW is the quadrupole term $\propto \epsilon^2$, which dominates the interaction for long distances, $L \gg 2r_c$. The presence of higher-order terms in the expansion (Table 1) is due to the fact that we deal with particles of finite size (Figure 3), rather than with "point quadrupoles".

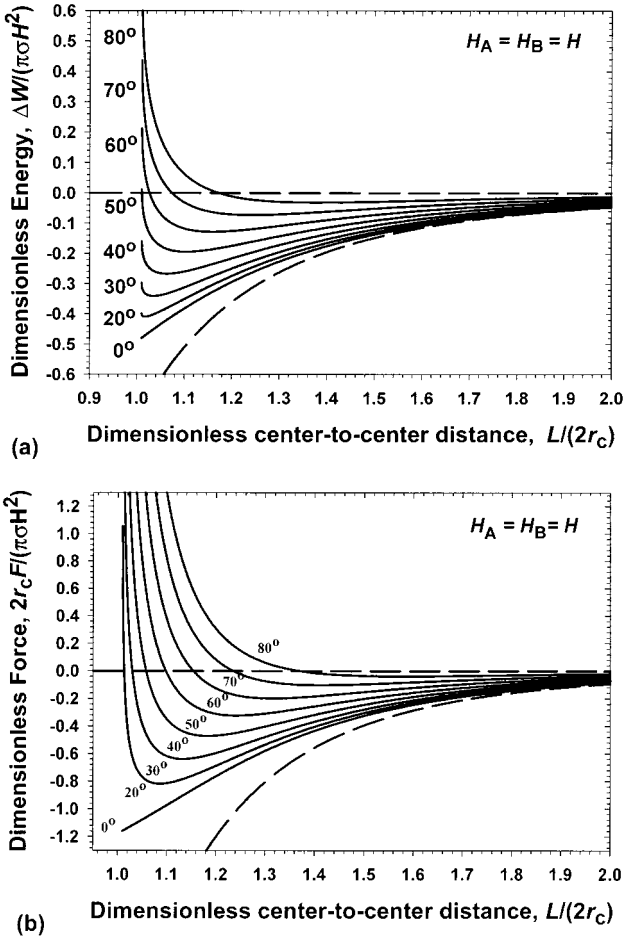

Figure 6. Plots (a) of the dimensionless energy of capillary interaction, $\Delta W/(\pi\sigma H^2)$, eq 3.17, and (b) of the dimensionless force $2r_cF/(\pi\sigma H^2)$, as functions of the dimensionless distance $L/(2r_c)$ between two similar particles: $H_A = H_B = H$. The different curves correspond to different values of the phase angle $\Delta\varphi$, denoted in the figure. The dashed curves correspond to the long-distance asymptotic expressions, eqs 4.10 and 5.10, for $\Delta\varphi = 0$.

4.2. Calculated Energy and Force. To calculate the exact dependence $\Delta W(L)$, we use eqs 3.17 and 3.20, along with eqs 4.2, 4.4, and 4.5. Figure 6a shows calculated energy versus distance curves for identical particles, $H_A = H_B = H$. The force versus distance curves in Figure

6b are obtained by numerical differentiation of the respective curves in Figure 6a. The different curves correspond to different values of the phase angle

$$\Delta\varphi = 2\varphi_A + 2\varphi_B \tag{4.11}$$

For $\Delta\varphi > 13°$, the dependence $\Delta W(L)$ exhibits a minimum; that is, the interaction is attractive at long distances, but repulsive at short distances (Figure 6a,b). In contrast, for $0 \le \Delta\varphi < 13°$, the interaction is attractive for all distances. This result for spherical particles qualitatively resembles the results of Lucassen[12] for cubic particles of an undulated contact line. However, for cubic particles, only the curve with $\Delta\varphi = 0$ has no minimum.[8,12] Lucassen's theory is approximate insofar as edge effects are neglected, while there are no edge effects for spherical particles, and in this respect our present theory is rigorous.

As seen in Figure 6, the interaction becomes more repulsive when the phase shift $\Delta\varphi$ increases. Consequently, the system of two particles (Figure 3) will tend to decrease $\Delta\varphi$ by spontaneous adjustment of the particle mutual orientation, to eventually achieve $\Delta\varphi = 0$. The global minimum of ΔW (the maximum attraction), corresponding to zero phase shift and close contact ($\Delta\varphi = 0$, $L = 2r_c$), is

$$\Delta W_{min} = \pi\sigma H^2[2S(0) - G(0) - 2] = -0.480552(\pi\sigma H^2) \tag{4.12}$$

(see eqs 3.17, 3.20, 4.6, and 4.7). For an emulsion-type interface, we take $\sigma = 5$ mN/m, and with $H = 10$ nm and $T = 25$ °C from eq 4.12, we estimate $\Delta W_{min} = 184kT$. This result demonstrates again that the energy of this type of capillary attraction can be very large as compared to the thermal energy kT, even for undulations of sub-micrometer amplitude. For example, this attractive force is able to cause aggregation of colloidal particles attached to the surface of emulsion drops.[16−18] This effect could be important also for the Pickering emulsions, that is, emulsions stabilized by adsorbed colloidal particles.[19−22]

It is curious to note that ΔW_{min} does not depend on r_c (i.e., on the particle size) at a fixed amplitude of undulation, H (see eq 4.12). In other words, the energy of capillary attraction at close contact is the same for particles−quadrupoles of size, say, 10 μm and 100 nm.

The lowest dashed lines in Figure 6a and b are calculated by means of the asymptotic expression 1.7 for $\Delta\varphi = 0$. One sees that the asymptotic formula becomes sufficiently accurate for $L/(2r_c) > 1.9$. Note that the asymptotic expression 1.7 does not describe the nonmonotonic behavior for smaller $L/(2r_c)$ and $\Delta\varphi > 13°$.

Figure 7a,b shows $\Delta W(L)$ and $F(L)$ dependencies, which have been calculated in the same way as those in Figure 6, but this time for $H_A \neq H_B$ and $\Delta\varphi = 0$. (Particles of different undulation amplitudes were used in some of the experiments on capillary interactions performed by Whitesides and co-workers.[9,10,18]) The different curves correspond to different fixed values of the ratio H_B/H_A. To specify the system, it is assumed that $H_B \ge H_A$. For $1 \le H_B/H_A < 1.2572$, the interaction is monotonic attraction. For $H_B/H_A > 1.2572$, the $\Delta W(L)$ curves exhibit a minimum, corresponding to an equilibrium distance between the two particles, which increases with the rise of H_B/H_A. On the other hand, at fixed H_A, the depth of the minimum is not very sensitive to the value of H_B.

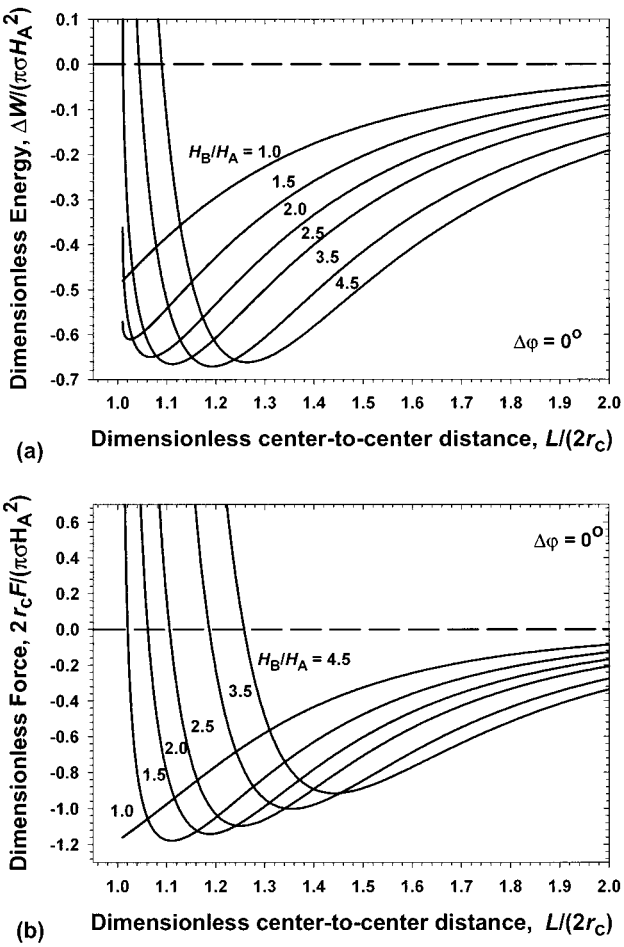

Figure 7. Plots (a) of the dimensionless energy of capillary interaction, $\Delta W/(\pi\sigma H_A^2)$, and (b) of the dimensionless force $2r_cF/(\pi\sigma H_A^2)$, as functions of the dimensionless distance $L/(2r_c)$ in the absence of phase shift, $\Delta\varphi = 0$. The different curves correspond to different fixed values of the ratio H_B/H_A, denoted in the figure.

5. Dilatational Deformation of Particulate Monolayers

5.1. Directed and Nondirected Interactions. In the previous sections, we investigated the interaction between two particles: capillary quadrupoles. Here we continue with the collective behavior (the rheological properties) of an adsorption monolayer of such particles at a fluid interface, for example, in a Langmuir trough.

We consider a system of identical particles−quadrupoles, for which $H_A = H_B$. Since all particles are treated as equivalent elements of a large two-dimensional array (negligible edge effects), we assume that all quadrupoles are oriented in the same direction, $\varphi_A = \varphi_B$ (cf. Figures 3 and 8a). The shape of the interaction−energy curves in Figure 6a implies that the particles will spontaneously move and rotate until forming an equilibrium two-dimensional square lattice with zero phase shift (Figure 8a).

(16) Velev, O. D.; Furusawa, K.; Nagayama, K. *Langmuir* **1996**, *12*, 2374.
(17) Velev, O. D.; Furusawa, K.; Nagayama, K. *Langmuir* **1996**, *12*, 2385.
(18) Huck, W. T. S.; Tien, J.; Whitesides, G. M. *J. Am. Chem. Soc.* **1998**, *120*, 8267.
(19) Pickering, S. U. *J. Chem. Soc.* **1907**, *91*, 2001.
(20) Tadros, Th. V.; Vincent, B. In *Encyclopedia of Emulsion Technology*; Becher, P., Ed.; Marcel Dekker: New York, 1983; Vol. 1, p 129.
(21) Denkov, N. D.; Ivanov, I. B.; Kralchevsky, P. A.; Wasan, D. T. *J. Colloid Interface Sci.* **1992**, *150*, 589.
(22) Thieme, J.; Abend, S.; Lagaly, G. *Colloid Polym. Sci.* **1999**, *277*, 257.

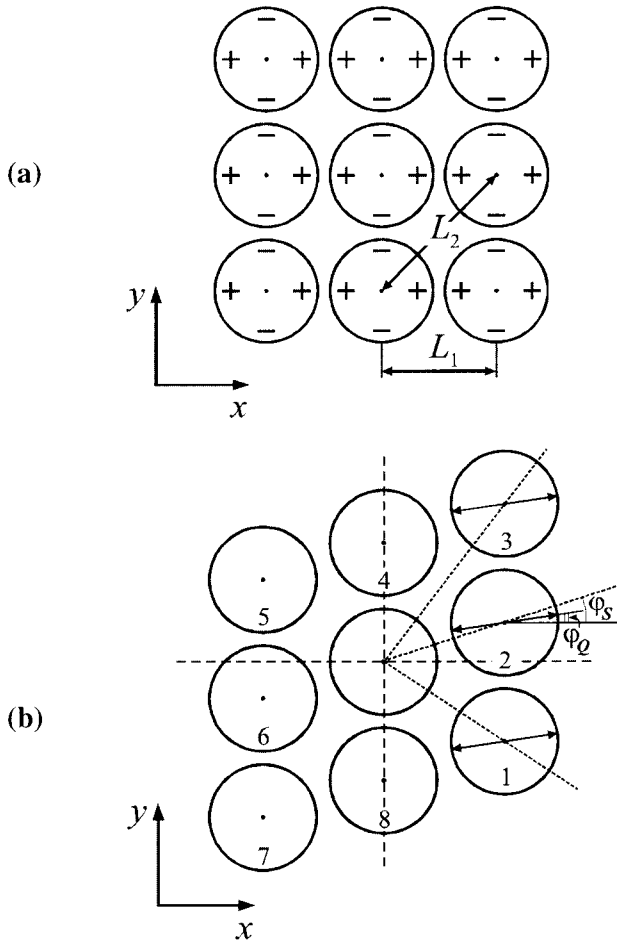

Figure 8. (a) Sketch of an equilibrium lattice of capillary quadrupoles; L_1 and L_2 are the distances between first and second neighbors in the lattice. (b) The same lattice after a shear along the y axis; the angles φ_S and φ_Q characterize, respectively, the shear and the quadrupole rotation.

It is natural to assume that in addition to the quadrupole−quadrupole capillary force, the particles also experience other types of interactions, which are independent of the particle rotation, for example, van der Waals and electrostatic forces and/or interaction between capillary charges. To distinguish the directed, orientation-dependent quadrupole interactions from the other non-directed interactions, we denote the former by a subscript "Q", and the latter by a subscript "ND". Since the latter two types of interactions have different physical origin, one could assume that the interaction energy and force between each couple of particles in the array are presented as a superposition of two terms

$$W(L,\varphi) = W_Q(L,\varphi) + W_{ND}(L); \qquad F(L,\varphi) = F_Q(L,\varphi) + F_{ND}(L) \quad (5.1)$$

5.2. Surface Pressure and Dilatational Elasticity. In this subsection, we consider isotropic dilatation of particulate monolayers. Our aim is to estimate the contribution of the quadrupole interactions to the two-dimensional surface pressure, Π, and to the dilatational elastic modulus, E_D (shear deformations are considered in section 6). For the sake of simplicity, we will first account only for the interaction of every particle with its first and second neighbors, viz. the closest four neighbors (situated at a distance L_1) and the diagonal four neighbors situated at a distance $L_2 = \sqrt{2}L_1$ (Figure 8a). The contribution of the other, more distant particles in the array is estimated in Appendix B.

By definition, the surface pressure is given by the expression

$$\Pi(A) = -\left(\frac{\partial\Omega}{\partial A}\right)_T \quad (5.2)$$

where Ω is the surface grand thermodynamic potential of the system, and A is the surface area. For adsorption monolayers of sufficiently large particles, the entropy contribution to Π is negligible; hence, Π can be expressed through the total particle−particle interaction energy:

$$\Pi(A_0) = -\frac{1}{2}\left(\frac{\partial W_T}{\partial A_1}\right)_T \quad (5.3)$$

Here $A_1 = L_1^2$ is the area per particle in the monolayer, and W_T is the total interaction energy of a given (arbitrarily chosen) particle with its neighboring particles. The multiplier $^1/_2$ appears in eq 5.3 to avoid a double counting of the interaction energy between two particles. Equation 5.3 shows that the various types of interparticle forces give additive contributions to Π, if they give additive contributions to the interaction energy, as it is in eq 5.1.

The isotropic compression and expansion of the particle array do not affect the orientation of the quadrupoles. In such a case, the differentiation in eq 5.3 is to be performed at a fixed orientation of the interacting quadrupoles. Thus, one derives

$$\Pi_Q(L_1) = -\frac{1}{4L_1}\left(\frac{\partial W_{QT}}{\partial L_1}\right)_{T,\varphi} = (F_1 + \sqrt{2}F_2)/L_1 \quad (5.4)$$

where W_{QT} is the total energy of the quadrupole−quadrupole interaction of a given particle with its neighbors; $F_1 = F_Q(L_1, \varphi = 0)$ and $F_2 = F_Q(L_2, \varphi = \pi/4)$ are the capillary forces between this particle and its first and second neighbors in the square lattice. It is convenient to define a dimensionless surface pressure

$$\tilde{\Pi}_Q(L_1) \equiv \Pi_Q\frac{4r_c^2}{\pi\sigma H^2} = \frac{2r_c}{L_1}(\tilde{F}_1 + \sqrt{2}\tilde{F}_2) \quad (5.5)$$

where

$$\tilde{F}_k \equiv \frac{2r_cF_k}{\pi\sigma H^2}; \quad k = 1,2 \quad (5.6)$$

is the respective dimensionless capillary force.

If the particles are in close contact, $L_1 \to 2r_c$, the capillary force can be calculated by numerical differentiation of eq 3.17, along with eqs 4.2, 4.4, and 4.5:

$$\tilde{F}_1(L_1 \to 2r_c) = -1.161...; \quad \tilde{F}_2(L_1 \to 2r_c) = 0.698... \quad (5.7)$$

Likewise, for the limiting value of the surface pressure at particle contact one obtains

$$\tilde{\Pi}_Q(L_1 \to 2r_c) \approx -0.174 \quad (5.8)$$

Taking into account the contribution of the more distant particles (see Appendix B), one can estimate the dimensionless surface pressure to be about −0.286. (Note that the contribution of the attractive capillary interactions to Π is negative.) Thus, one can estimate that for particles with $(H/r_c)^2 \approx 0.1$ and $\sigma \approx 70$ mN/m, $\Pi_Q \approx -1.6$ mN/m.

The use of the asymptotic expression, eq 4.10, for the calculation of F_2 leads to

$$\Pi_Q(L_1) = \left[F_1 + \frac{3\pi\sigma}{8}\frac{H^2}{r_c}\left(\frac{2r_c}{L_1}\right)^5\right]/L_1 \qquad (5.9)$$

or in a dimensionless form

$$\tilde{\Pi}_Q(L_1) = \frac{2r_c}{L_1}\left[\tilde{F}_1 + \frac{3}{4}\left(\frac{2r_c}{L_1}\right)^5\right] \qquad (5.9a)$$

If the lattice constant is significantly larger than the particle diameter ($L_1 > 3r_c$), one can use eq 4.10 for calculation of the force F_1; thus, one obtains the following asymptotic results:

$$\tilde{F}_1 \equiv -3\left(\frac{2r_c}{L_1}\right)^5 \qquad (L_1 > 3r_c) \qquad (5.10)$$

$$\tilde{\Pi}_Q(L_1) \equiv -\frac{9}{4}\left(\frac{2r_c}{L_1}\right)^6 \qquad (L_1 > 3r_c) \qquad (5.11)$$

which show that the surface pressure rapidly decreases with the interparticle separation, L_1.

From the surface pressure, Π, one can calculate the contribution of the quadrupole interaction in the dilatational elasticity, E_D, of the particle layer:

$$E_D \equiv -\frac{d\Pi}{d\ln(A)} = -\frac{L_1}{2}\frac{d\Pi}{dL_1} \qquad (5.12)$$

The following asymptotic expression at a large interparticle separation can be derived from eqs 5.5, 5.11, and 5.12:

$$E_D = -\frac{45\pi}{32}\frac{\sigma H^2}{r_c^2}\left(\frac{2r_c}{L_1}\right)^6 \qquad (L_1 \geq 3r_c) \qquad (5.13)$$

For smaller interparticle separations, E_D can be found by numerical differentiation of the expressions for the force, $F_Q(L)$ (see eqs 5.4 and 5.12). The contribution of the capillary force in Π and E_D is negative, because this force is attractive.

5.3. Elasticity upon Unidirectional Dilatation. We consider a particle square array, which is a two-dimensional (2-D) crystal. In other words, we accept that it behaves as a 2-D elastic body rather than as a 2-D fluid. In such a case, one could imagine a process of unidirectional compression of the 2-D crystal along one of its axes. For example, if one of the crystal axes is parallel to the barrier of a Langmuir trough, then a displacement of the barrier would lead to a unidirectional deformation of the array. In general, the surface stress is expected to be different in the cases of isotropic and unidirectional deformations. In the latter case, the surface stress (force per unit length of the barrier) is

$$\tau = F_{QP}/L_1 \qquad (5.14)$$

where F_{QP} is the projection (along the normal to the barrier) of the capillary force acting on a given particle. Taking into account only the closest neighbors, situated at distances L_1 and L_2, one derives

$$F_{QP} = F_1 + 2|F(L_2)|\cos(\pi/4) \approx F_1 + \sqrt{2}F_2 \qquad (5.15)$$

which gives an expression for τ, which is equivalent to eq 5.4 for Π_Q:

$$\tau \approx \Pi_Q \approx (F_1 + \sqrt{2}F_2)/L_1 \qquad (5.16)$$

Therefore, one can use the various expressions derived for Π_Q, eqs 5.5−5.11, to estimate τ. Note, however, that τ and Π_Q are, strictly speaking, nonidentical quantities, and if one takes into account the interactions with more distant particles (behind the closest neighbors), a small numerical difference between τ and Π_Q appears (see Appendix B).

5.4. Yield Stress. If the particles interact only through a quadrupole capillary interaction, they will spontaneously form a close-packed square lattice; then $L_1 = 2r_c$. If we try to separate the particles by an external stress, they will resist the lattice deformation until the applied stress exceeds the attractive capillary force. According to eq 5.16, one can estimate the value of the stress, that should be overcome, as

$$\tau^* = \frac{\pi\sigma H^2}{4r_c^2}(\tilde{F}_1 + \sqrt{2}\tilde{F}_2) \approx -0.174\frac{\pi\sigma H^2}{4r_c^2} \qquad \text{(yield stress)} \qquad (5.17)$$

The account for the more distant particles leads to a larger magnitude of the dimensionless yield stress, −0.215 (see Appendix B). After this yield stress is exceeded, the interparticle forces are no longer able to counterbalance the applied external stress, and the monolayer will be disrupted. This is a typical plastic behavior[23] characterized by the value of the yield stress τ^*. Equation 5.17 shows that τ^* increases when the undulations' amplitude H increases and/or when the particle radius r_c decreases. With $(H/r_c)^2 = 0.1$ and $\sigma = 70$ mN/m, one estimates $\tau^* \approx 1.2$ mN/m.

6. Shear Deformation of Particulate Monolayers

Figure 8b shows a small shear deformation along the y axis characterized by the shear angle φ_S. This shear leads to a rotation of the quadrupoles to a given angle (with respect to their initial orientation), which will be denoted by φ_Q. In general, $\varphi_S \neq \varphi_Q$. Since the particles have identical environments, it is natural to assume that the angle of rotation, φ_Q, is the same for all of them; φ_Q can be found by minimization of the total interaction energy between the particles, $W_{QT}(L_1, \varphi_S, \varphi_Q)$:

$$\left.\frac{\partial W_{QT}}{\partial \varphi_Q}\right|_{\varphi_S, L_1} = 0 \qquad (6.1)$$

As before, we will use the approximation that W_{QT} includes the contribution of the eight closest neighbors of each given particle. In Appendix C, we demonstrate that eq 6.1 leads to a linear relation between the angles φ_S and φ_Q

$$\varphi_Q = \beta\varphi_S; \quad \beta = \frac{G_1 - \sqrt{2}G_2}{2(G_1 - G_2)} \qquad (6.2)$$

where the functions $G_1 = G(L_1)$ and $G_2 = G(L_2)$ are defined by eqs 4.2 and 4.5. For a large lattice constant (see eqs 4.3 and 4.9), one obtains

(23) Shchukin, E. D.; Pertsov, A. V.; Amelina, E. A. *Colloid Chemistry*; Moscow University Press: Moscow, 1982 (Russian Edition); Elsevier: Amsterdam, 2001 (English Edition).

$$G_1 \approx 12\left(\frac{r_c}{L_1}\right)^4; \quad G_2 \approx 12\left(\frac{r_c}{L_2}\right)^4 = 3\left(\frac{r_c}{L_1}\right)^4 \qquad (L_1 \gg 2r_c) \tag{6.3}$$

which leads to

$$\beta \approx 2/3 - \sqrt{2}/6 \approx 0.431 \qquad (L_1 \gg 2r_c) \tag{6.4}$$

On the other hand, for particles at close contact the numerical summation in eq 4.5 yields

$$G_1 \approx 1.6975; \quad G_2 \approx 0.19242; \quad \beta \approx 0.474; \quad \text{at } L_1 = 2r_c \tag{6.5}$$

In view of eq 6.2, these estimates show that the quadrupoles rotate at an angle which is about one-half of the shear angle, φ_S.

Following the thermodynamic approach by Landau and Lifshitz,[24] one can determine the shear elastic modulus, E_S, by differentiation of the free energy of the system with respect to the shear deformation (see eq 4.1 in ref 24). In our notation, this relation reads

$$E_S = \frac{1}{2u_{yx}}\frac{\partial \Omega}{\partial u_{yx}} = \frac{1}{\varphi_S L_1^2}\frac{\partial W_{QT}}{\partial \varphi_S}\bigg|_{\varphi_Q = \beta\varphi_S} \tag{6.6}$$

where the coefficient of surface shear elasticity, E_S, is a 2-D analogue of the coefficient of Lamé, μ, in ref 24. For small shear angles, the relative displacement along the y axis, $u_{yx} = (\partial u_y/\partial x)/2$, is equal to $\varphi_S/2$. The differentiation of W_{QT} in eq 6.6 leads to the following expression for E_S (see Appendix C):

$$E_S = 32\pi\sigma\left(\frac{H}{L_1}\right)^2\{G_1[(\beta - 1)^2 + \beta^2] - G_2(\sqrt{2}\beta - 1)\} \tag{6.7}$$

With the help of eqs 6.3, 6.4, and 6.7 for large interparticle distances, one derives

$$E_S = 8.88\sigma\left(\frac{H}{r_c}\right)^2\left(\frac{2r_c}{L_1}\right)^6 \qquad (L_1 \gg 2r_c) \tag{6.8}$$

Likewise, using eqs 6.5 and 6.7, for particles in contact, one derives

$$E_S = 23\sigma\left(\frac{H}{r_c}\right)^2 \qquad (L_1 = 2r_c) \tag{6.9}$$

These estimates show that for $\sigma = 70$ mN/m and $H/r_c = 0.1$, E_S is on the order of 16 mN/m.

7. Summary and Conclusions

The interfacial deformations, which give rise to the lateral capillary forces, are characterized by capillary charges (section 1.1). In the case of particles with an undulated contact line, the convex and concave local deviations of the meniscus shape from planarity can be treated as positive and negative capillary charges, which form capillary multipoles. Correspondingly, the meniscus shape can be expressed as a multipole expansion (eq 1.6). The dominant terms of the capillary multipole expansion are the charges and quadrupoles, with the dipoles being spontaneously annihilated by the fluid interface.[13]

In the present article, we derive theoretical expressions allowing one to calculate the energy and force of interaction between two capillary quadrupoles for an arbitrary distance, L, between them (see eqs 3.17, 4.4, and 4.5). Depending on the amplitudes of the contact-line undulations and on the particle mutual orientations, the interaction is either monotonic attraction or it is attraction at long distances but repulsion at short distances (see Figures 6 and 7). As a rule, the interaction energy is much larger than the thermal energy kT, even for contact-line undulations of nanometer amplitudes (see eq 4.12). For that reason, the forces between capillary multipoles do certainly influence many phenomena with particles at fluid interfaces, although these effects have been practically unexplored so far.

On the basis of the results for the interaction energy, one can predict the rheological behavior of adsorption monolayers from capillary quadrupoles when subjected to dilatational and shear surface deformations (Figure 8). It turns out that an equilibrium monolayer of identical particles exhibits plastic behavior upon dilatation; an expression for the respective yield stress is derived (eq 5.17). Expressions for the contributions of the capillary interactions to the surface dilatational and shear modules of elasticity are derived (see eqs 5.4, 5.12, 6.7, and Appendix B).

The results of this paper could be helpful for the understanding of some phenomena related to the aggregation and the ordering of particles adsorbed at a fluid interface and for interpretation of the rheological behavior of monolayers from such particles. For example, related research fields are Pickering emulsions and two-dimensional ordered arrays of microscopic particles.

Appendix A: Derivation of Eq 3.14

Using the identity $\cos(\varphi) = \pm(1 - \sin^2(\varphi))^{1/2}$, from eq 3.13 one obtains

$$\cos(\varphi) = \pm\frac{\cosh(\tau_c)\cos(\omega) - 1}{\cosh(\tau_c) - \cos(\omega)} \qquad (-\pi \le \omega \le \pi) \tag{A.1}$$

Here, and hereafter, the upper and lower sign, "±", refers, respectively, to the right- and left-hand side particle (Figure 3). To determine A_n, we start from the identity $\cos(2\varphi) = 2\cos^2(\varphi) - 1$, in which we substitute $\cos(\varphi)$ from eq A.1. Next we use the identity

$$\cosh(\tau_c)\cos(\omega) - 1 = (\cos(\omega) - \cosh(\tau_c))\cosh(\tau_c) + \sinh^2(\tau_c) \tag{A.2}$$

and insert the resulting expression for $\cos(2\varphi)$ into eq 3.12. Thus, we obtain

$$A_n = -4I(\tau_c)\cosh(\tau_c)\sinh^2(\tau_c) - 2(\mathrm{d}I/\mathrm{d}\tau_c)\sinh^3(\tau_c) \tag{A.3}$$

where

$$I(\tau_c) = \int_{-\pi}^{\pi}\frac{\cos(n\omega)\,\mathrm{d}\omega}{\cosh(\tau_c) - \cos(\omega)} \tag{A.4}$$

With the help of mathematical tables,[25] one can derive

$$I(\tau_c) = \frac{2\pi\exp(-n\tau_c)}{\sinh(\tau_c)} \tag{A.5}$$

(24) Landau, L. D.; Lifshitz, E. M. *Theory of Elasticity*; Pergamon Press: Oxford, 1970.

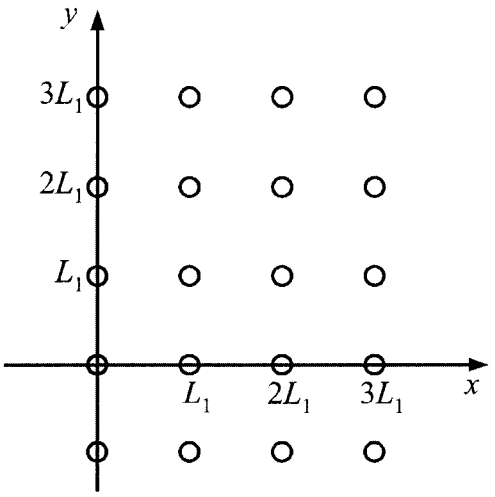

Figure 9. Derivation of the contribution of the distant particles to the surface pressure (see the text).

The substitution of eq A.5 into A.3, after some transformations, yields the expression for A_n in eq 3.14.

To determine B_n, we start from the identity $\sin(2\varphi) = 2\cos(\varphi)\sin(\varphi)$, in which we substitute $\cos(\varphi)$ from eq A.1 and $\sin(\varphi)$ from eq 3.13. Next we use again eq A.2 and insert the resulting expression for $\sin(2\varphi)$ into eq 3.12. Thus, we obtain

$$-B_n = \pm[2\,J(\tau_c)\cosh(\tau_c)\sinh(\tau_c) + 2(\mathrm{d}J/\mathrm{d}\tau_c)\sinh^2(\tau_c)] \tag{A.6}$$

where

$$J(\tau_c) = \int_{-\pi}^{\pi} \frac{\sin(\omega)\sin(n\omega)\,\mathrm{d}\omega}{\cosh(\tau_c) - \cos(\omega)} \tag{A.7}$$

With the help of mathematical tables,[25] one can derive

$$J(\tau_c) = 2\pi\exp(-n\tau_c) \tag{A.8}$$

The substitution of eq A.8 into A.6, after some transformations, yields the expression for B_n in eq 3.14.

Appendix B: Contribution of the Distant Particles to the Surface Pressure

In the main text, we considered only the capillary interaction of a given particle with its first and second neighbors situated, respectively, at distances L_1 and $L_2 = \sqrt{2}L_1$. The contribution of the remaining, more distant particles to the surface pressure and dilatational elasticity of the layer can be estimated if one assumes that they interact with the central particle by the asymptotic expression, eq 4.10.

Let us consider a square lattice with constant L_1, like that shown in Figure 9. One can extend eq 5.4 to include the interactions of a given particle with all particles in the 2-D array:

$$\Pi_Q(L_1) = \frac{1}{4L_1}\sum F_Q(L,\varphi)\frac{\mathrm{d}L}{\mathrm{d}L_1} \tag{B.1}$$

The summation is carried out with respect to all discrete values of the distance L between the given particle and all its neighbors in the lattice. Equation B.1 can be transformed to read

$$\Pi_Q = \frac{1}{L_1}(F_1 + \sqrt{2}F_2) - \frac{3}{4}\pi\sigma\left(\frac{H}{L_1}\right)^2\left(\frac{2r_c}{L_1}\right)^4\sum\cos(4\varphi)\left(\frac{L_1}{L}\right)^4 \tag{B.2}$$

where the summation now is carried out over all particles except the first and the second neighbors, which are accounted for by the terms with F_1 and F_2. If we introduce dimensionless coordinates m and n for the particles, along the x and y axes (see Figure 9), then

$$L/L_1 = (m^2 + n^2)^{1/2} \tag{B.3}$$

$$\cos(4\varphi) = \cos\left[4\,\arccos\left(\frac{m}{\sqrt{m^2+n^2}}\right)\right] = \frac{8m^4}{(m^2+n^2)^2} - \frac{8m^2}{(m^2+n^2)} + 1 \tag{B.4}$$

The substitution of eqs B.3 and B.4 into eq B.2 and the summation over the distant particles lead to the following result for the contribution of the quadrupole interactions to the surface pressure of the particle monolayer:

$$\Pi_Q = \frac{1}{L_1}(F_1 + \sqrt{2}F_2) - 3\pi\sigma\left(\frac{H}{L_1}\right)^2\left(\frac{2r_c}{L_1}\right)^4\left[\left(\frac{\pi^4}{90} - 1\right) - 0.045\right] = \frac{1}{L_1}(F_1 + \sqrt{2}F_2) - 0.112\pi\sigma\left(\frac{H}{L_1}\right)^2\left(\frac{2r_c}{L_1}\right)^4 \tag{B.5}$$

In dimensionless form, the surface pressure can be presented as

$$\tilde{\Pi}_Q = \Pi_Q\frac{4r_c^2}{\pi\sigma H^2} = \frac{2r_c}{L_1}\left[\tilde{F}_1 + \sqrt{2}\tilde{F}_2 - 0.112\left(\frac{2r_c}{L_1}\right)^5\right] \tag{B.6}$$

Equation B.7 predicts that at closest contact of the particles, $L_1 = 2r_c$, the dimensionless surface pressure is $\tilde{\Pi}_Q \approx -0.286$ (see also eq 5.7).

In a similar way, one can calculate the contribution of the distant neighbors in the stress related to a unidimensional deformation:

$$\tau = \frac{1}{L_1}(F_1 + \sqrt{2}F_2) - \frac{\pi\sigma H^2}{L_1 r_c}\frac{3}{2}\left(\frac{2r_c}{L_1}\right)^5\sum\cos(4\varphi)\left(\frac{L_1}{L}\right)^5\frac{m}{\sqrt{m^2+n^2}} \tag{B.7}$$

where the summation is over the particles with coordinate $x > 0$. The final result reads

$$\tilde{\tau} = \tau\frac{4r_c^2}{\pi\sigma H^2} = \frac{2r_c}{L_1}\left[\tilde{F}_1 + \sqrt{2}F_2 - 0.041\left(\frac{2r_c}{L_1}\right)^5\right] \tag{B.8}$$

which predicts for a layer of closely packed particles $\tilde{\tau} = -0.215$.

Appendix C: Shear Deformation and Shear Elasticity

Here we derive eqs 6.2 and 6.7. The interaction energy W_{QT} of a given particle with its eight closest neighbors in the monolayer, which is subjected to a small shear deformation, is (see eq 6.1)

(25) Prudnikov, A.; Brychkov, Y.; Marichev, O. *Integrals and Series*; Gordon & Breach: Newark, NJ, 1996; Vol. 1.

$$W_{QT} = 2(W_1 + W_2 + W_3 + W_4) \qquad \text{(C.1)}$$

where W_k is the interaction energy with particle k, as indicated in Figure 8b. The multiplier 2 in eq C.1 comes from the symmetry of the system, which implies that the interaction with particles 1 and 5, 2 and 6, 3 and 7, and 4 and 6 are equivalent.

From eq 3.17 and Figure 8b, one can express the respective interaction energies as

$$W_1 = \pi\sigma H^2\left\{2S_2 - G_2\cos\left[4\left(\frac{\pi}{4} + \varphi_Q - \varphi_S/\sqrt{2}\right)\right]\right\} \qquad \text{(C.2)}$$

$$W_2 = \pi\sigma H^2\{2S_1 - G_1\cos[4(\varphi_Q - \varphi_S)]\} \qquad \text{(C.3)}$$

$$W_3 = \pi\sigma H^2\left\{2S_2 - G_2\cos\left[4\left(\frac{\pi}{4} - \varphi_Q + \varphi_S/\sqrt{2}\right)\right]\right\} \qquad \text{(C.4)}$$

$$W_4 = \pi\sigma H^2[2S_1 - G_1\cos(4\varphi_Q)] \qquad \text{(C.5)}$$

where, using eqs 4.1, 4.2, 4.4, and 4.5, we have defined

$$S_1 = S(L = L_1) \quad \text{and} \quad G_1 = G(L = L_1) \qquad \text{(C.6)}$$

$$S_2 = S(L = L_2) \quad \text{and} \quad G_2 = G(L = L_2) \qquad \text{(C.7)}$$

which do not depend on the shear angle, φ_S, or on the angle of quadrupole phase rotation, φ_Q (see Figure 8b).

The substitution of eqs C.2−C.5 into eq 6.1 and the subsequent differentiation lead to eq 6.2. Respectively, the substitution of eqs C.2−C.5 into eq 6.6 leads to eq 6.7. Note that the relative change of the interparticle distance upon shear is a higher-order effect at small φ_S, because it is proportional to φ_S^2.

LA0109359